Academia Journal of Medicinal Plants X(X): 000-000, XXXXX 2018
DOI: 10.15413/ajmp.2018.0XXX
ISSN 2315-7720

Academia Publishing

Research Paper

Evaluation of the effects of *Ulva* sp., *Cryptomenia* sp., *Ciona intestinalis* and *Heliotropium* sp. crude extracts as possible interfering agents on the Autophagocytosis pathway: Preliminary results

Bernardini S[1], Donoso-Fierro C[2], Tiezzi A[1], Tassoni M[3], Fava E[3], Becerra J[2], Perez C[2]* and Ovidi E[1]

[1]Dipartimento per la Innovazione nei Sistemi Biologici Agroalimentari e Forestali (DIBAF), Università degli Studi della Tuscia, Largo dell'Università snc, Viterbo, Italy.
[2]Laboratorio de Química de Productos Naturales, Departamento de Botánica, Facultad de Ciencias Naturales y Oceanográficas, Universidad de Concepción, Concepción, Barrio Universitario s/n, PO box 160-C, Concepción.
[3]DZNE - German Center for Neurodegenerative Diseases, Sigmund Freud Strasse, 27 53175 Bonn, Germany.

Accepted Date

ABSTRACT

In the current drug discovery landscape, natural products continue to be the most important source of new drugs. Research efforts have focused on the development of drugs against pathologies that still lack effective therapeutic treatments. In this context, a cellular process that is physiologically involved in the maintenance of cellular homeostasis, referred to as autophagy, has emerged in recent decades for its involvement in the onset of many diseases. Recent studies have aimed to discover new molecular entities from natural sources that are able to interfere in this process and prevent the onset of pathologies such as cancer, infection and neurodegenerative diseases. In the present study, an approach consisting of cell-based assays, followed by a High Content Analysis, has been specifically developed and fine-tuned to select the most interesting crude natural extracts in terms of their effects on the autophagy process. In particular, the analysis of the 40 starting samples derived from 5 crude extracts allowed the isolation of 22 samples, which were sorted based on different typologies of interference on the autophagy process.

Key words: Autophagy, natural products, crude extracts, Autophagocytosis, cell-based assays.

Abbreviations: HCS, High-content screening; **PCA,** principal component analysis; **HCA,** hierarchical cluster analysis; **LC3 protein,** microtubule associated proteins light chain 3; **PFA,** paraformaldehyde; **PC,** principal component; **PBS 1X,** phosphate-buffered saline; **BSA,** bovine serum albumine; **DMSO,** dimethyl sulfoxide

INTRODUCTION

Many of the pathologies affecting humans, such as cancer, neurodegenerative diseases, cardiac affections and diabetes still require efficient pharmacological interventions. Considering that more than 95% of the world's biodiversity has not been evaluated for any biological activity, natural products that originate from Earth's bio-diverse flora and fauna represent an important reservoir for novel molecular entities that can be introduced to the drug discovery pipeline, as has already been reported (Abdi, 2010; Abraham et al., 2004; Alessi and Downes, 1998). In this context, plants, as well as the associated microflora, represent a wide source of new molecules potentially containing pharmaceutical properties.

The characterization of such molecules should be performed using the appropriate research techniques, primarily consisting of cell-based assays (Arroyo et al., 2014; ATCC, 2014; Bhutia et al.,2013; Bravo-San Pedro et al., 2017; Carnero, 2006), which improve the quality of lead

candidates (Carpenter et al., 2006). An emerging functional, cell-based and multiplexed technology was utilized, known as High-Content Screening (HCS) (Cuervo, 2004; De Vorkin and Gorski, 2014; Dewick, 2009), through which the effects of the treatments in cellular systems were examined by detecting different phenotypical features simultaneously, which can lead to the discovery of new drugs derived from natural products. A powerful property of HCS is that potency, selectivity and cytotoxicity can all be determined in a single assay. Currently, HCS based drug discovery programs are primarily focused on searching for therapeutic protein or small molecules involved in the treatment of diseases "currently lacking" effective drugs, such as neurological disorders and autoimmune diseases (Carpenter et al., 2006).

The current scientific research landscape proposes that perturbations of the basal conditions of the autophagy process are involved in the onset of pathological conditions, which can lead to the development of the most common diseases and disorders of the modern age, such as cancer, neurodegeneration, aging, metabolic syndrome, inflammatory disorders and cardiovascular diseases (Eskelinen, 2008; Fitzwalter and Thorbun, 2015; Geng and Klionsky, 2008; Giuliano et al., 2003; Glick et al., 2010; Gribbon and Sewing, 2003). Autophagy is a strictly regulated and evolutionarily conserved physiological cellular pathway for the digestion of damaged cytoplasmic materials or aged organelles. The process consists of enveloping intracellular materials into double layered membrane structures named "autophagosomes", which subsequently fuse with lysosomes to form new functional structures named "autophagolysosomes", in which digestion occurs (Johnston and Johnston, 2002; Kabeya et al., 2000; Kamentsky et al., 2011; Kirisako et al., 2000; Klionsky, 2007; Klionsky, 2005; Klionsky et al., 2016; Kundu and Thompson, 2008). During this process, autophagosomes move along cytoskeleton elements through LC3 protein (Atg8), which is considered to be the most common marker to monitor autophagy (Glick et al., 2010; Lamprecht et al., 2007; Lin and Baehrecke, 2015). LC3 protein exists in two different isoforms: LC3B I (14 KDa), a free cytosolic protein, and LC3B II (16 KDa), a protein present in the inner and outer membrane of autophagosomes. These two isoforms are alternated during the autophagy process: LC3B I is present in the basal condition and is converted into LC3B II during the formation of the autophagosomes. Then, when the autophagosome fuses with the lysosome, the LC3B II isoform is degraded by lysosomal activity (Ljosa and Carpenter, 2009; Mei et al., 2015; Mishra and Tiwari, 2011; Mizushima, 2004).

In this study, we present an HCS approach based on fluorescence and immunofluorescence assays developed for the evaluation and quantification of biological effects, for short and long time durations (2 and 20 h), on the extracts of four organisms among algae, invertebrate and plants on acidic and autophagosomal compartments, which are considered to be descriptive of autophagic activity (Levine and Kroemer, 2008; Lin and Baehrecke, 2015; Mizushima and Klionsky, 2007; Mizushima et al., 2010; Molyneux et al., 2007). Following the methods previously described in the literature (Lin and Baehrecke, 2015) and using an automated confocal microscope, it was possible to capture images regarding lysosomes in living treated cells in order to examine possible effects on the cellular acidic compartments, as well as LC3B in the same cells after fixation to study the effects on autophagic compartments. The obtained images were then analyzed, and quantitative data extracted from the images were used to determine specific parameters related to such cellular compartments. This approach allowed a qualitative and quantitative evaluation of the effects of the extracts on cells under physiological and autophagy-induced conditions.

MATERIALS AND METHODS

Sample collection and extract preparations

The marine samples *Ulva* sp., *Cryptonemia* sp., *Stenogramme* sp. and *Ciona* sp. were collected through an apnea dive from the culture lines of the submarine facilities of the Universidad Católica del Norte, located in the Herradura Bay, IV Region, Province of Elqui, Coquimbo, Chile (29° 57'S–71°21'W). The samples were washed with sterile seawater and 30% ethanol to remove any associated microflora, and washed again with fresh water to remove surface salts and sand particles. *Heliotropium* sp. was collected in the Coastal Mountains of Coquimbo (20 m.a.s.l.) (29° 59'S–71°21'W). All samples were left to dry in a shady and aerated placeto constant weight. To obtain the extracts, 50 g of each dried sample were weighed, ground and macerated in 150 mL of 99.89% ethanol to exhaustion at 40°C. The samples were filtered and concentrated under vacuum at 40°C. Thereafter, successive extractions were performed with solvent sorted by increasing polarity such as hexane, chloroform and ethyl acetate (4×100 mL). The resulting fractions were concentrated and stored at -40°C until use.

Cell model

Each experiment was conducted on SH-SY5Y cells. The culturing medium used to grow SH-SY5Y cells composed of a 1:1 mixture of ATCC-formulated Eagle's Minimum Essential Medium and an F-12 medium supplemented with 1% Sodium Pyruvate (#11360070, Thermo Fisher Scientific), 1% PenStrep (#15070063, Thermo Fisher Scientific) and 10% Fetal Bovine Serum (#26140079, Thermo Fisher Scientific). Common culturing conditions for SH-SY5Y cells are 95% air, 5% CO_2 and 37°C. All other

information about the handling of the SH-SY5Y cells was taken from the ATCC website (Monks et al., 1991).

For our study, SH-SY5Y cells were selected because it is considered a good neuronal model for analyzing the autophagy pathway.

Cells treatment with extracts

Dried extracts were weighed and resuspended in 100%dimethyl sulfoxide (#D5879, Sigma Aldrich) at a concentration of 100 mg/mL. Then, solutions were shaken for 1 h on vortex and left at 4°C overnight. The extracts were then diluted in a complete culturing medium and in a partially serum-deprived culturing medium (1% FBS) to the final concentration of 0.1 mg/mL in 0.1% dimethyl sulfoxide. The partially serum-deprived medium was used to keep the cells in starvation conditions, which is the most common method for inducing autophagy.

The obtained solutions were administered to the cells in four serial concentrations, from 0.1 mg/mL down to 0.01 mg/mL, and subjected to incubation for 2 and 20 h.

Fluorescence and immunofluorescence assays on living SH-SY5Y cells

The SH-SY5Y cells were seeded in 384-well plates at a concentration of 8×10^3 cells/well and, after 15-20 h of incubation, were treated as explained. Fluorescence assays on SH-SY5Y living cells were performed by adding a staining solution consisting of 100 nMLysotracker Red(#L-7528,TermoFisher Scientific) (Mizushima et al., 2010) and 100 nM Hoechst 33342 (#B2261, Sigma-Aldrich) 30 min before the end of the treatments. After 30 min in an incubator (37°C, 5% CO_2), the staining solutions in each sample were replaced with media and the cells were immediately scanned by the automated confocal microscope "Cell Voyager 6000" (Yokogawa), which obtained images in 9 different fields for each well.

After live imaging, cells were immediately fixed using a solution of 4% PFA (#10010023, Gibco) in PBS 1X for 5-10 min in the dark. Thereafter, the cells were permeabilized in a solution containing 0.1% digitonin (#D141, Sigma-Aldrich) in PBS 1X for 5 min in the dark. After permeabilization, blocking buffer solution consisting of 5% BSA in PBS 1X was added to the cells for 30 min in the dark, and then a 2.5 µg/ml of an anti-LC3B polyclonal antibody developed in rabbit (#L7543, Sigma-Aldrich), diluted in blocking buffer, was added in the wells and left in the dark for 45 min. Primary antibody solution was then removed, and cells were left in incubation with a solution containing 2 µg/ml Donkey anti-Rabbit IgG (H+L) Secondary Antibody Alexa Fluor® 488 conjugate (#A-21206, ThermoFisher Scientific), diluted in blocking buffer for 50 min. After incubation, a secondary antibody solution was replaced with PBS 1x and plates immediately scanned by the automated confocal microscope "Cell Voyager 6000" (Yokogawa), obtaining images in 9 different fields for each well. All tests were carried out at room temperature.

The automated confocal microscope and the image acquisition strategy

Images were collected by automated confocal microscopy using the Cell Voyager 6000 (Yokogawa©, Meters and Instruments Corporation, Japan), which acquires images from cells cultured in multi-well microplates using up to four different channels simultaneously. The CV6000 uses a high-resolution spinning disk confocal method and EMCCD cameras that allow an optimal signal-to-noise ratio. Images were acquired from both living and fixed cells, and the acquisition of the images of living cells was possible because the microscope was equipped with an incubator that maintains cells under a culturing condition (37°C; 5% CO_2). Four different channels (405, 448, 531 and 635 nm lasers) were selected according the fluorochromes used for each target and, before the images acquisition, the best focal plane was established by checking among those acquired every 2 µm.

Image analysis

Image analysis was performed using the CellProfiler software, a tool for quantifying data from biological images, particularly in high-throughput experiments (Nichols, 2007; Padmanabhan et al., 2010). The software requires the establishment of a "pipeline", or a sequential series of modules performing different image processing functions such as illumination correction, object identification (segmentation) and object measurement (Petibone et al., 2016). Moreover, CellProfiler, made it possible to distinguish different cell populations (such as living and dead cells), when working on particular measured features such as size, shape or intensity values of the previously identified objects (Pierzyńska-Mach et al., 2014). For each stained cellular element, a series of parameters were set and different algorithms were provided by the software to interpret the cellular elements depending on the cell type. Following some examples of these features, identification parameters, strategy and algorithms in SH-SY5Y cells were reported: nuclei were identified by considering all objects with a diameter between 40 and 150 pixels in the images revealed by the first channel (laser 405 nm: Hoechst 33342), while for Lysosomes and LC3B spots, such range was decreased to 5 to 15 pixels in the images revealed by the second channels (laser 531 nm: Lysotracker Red for Lysosomes; laser 488 nm: anti-LC3B polyclonal antibody for LC3B proteins). The strategies used to identify such objects were different depending on the different sizes and

distributions of the nuclei and the spots into the images, consisting of a global strategy (each image was analyzed entirely) for nuclei identification and an adaptive strategy (each image was divided into different fields and analyzed field by field for spots identification). Both nuclei and lysosomes/LC3B protein were filtered to discard possible background and artefacts signals by applying a minimum and a maximum threshold value (nuclei max 0.114 and min -; for spots max 0.1 and min 0.05) based on the upper quartile of the measured intensities of the signals detected. Cell boundaries were identified by "expanding" the signal detected for the nuclei for a defined number of pixels, determined by cell type. Moreover, the software assigns to each cell the exact number of spots, and provides a number for each cell among the output.

As the last step of the process, numerical values of the measurements were exported and were then used to interpret the phenotypes produced by the treatments.

Data normalization, principal component analysis (PCA) and hierarchical cluster analysis (HCA)

Data from the image analysis were selected and normalized by applying the Z-score or Standard Score to the median values from the measured features. The normalization step is needed in order to limit the effects of possible outlier values, as well as to make the measurements of parameters represented by values of different sizes comparable (percentages, number per cell and size).

PCA was then applied to the normalized values in order to reduce the dataset dimensions, and to reproduce only the most significant amount of variance in a number of variables of lower or equal to what was contained in the original dataset. In the present study, the PCA has been applied by decomposing a data matrix, after median centering, for each attribute using Z-scores (Sezgin and Sankur, 2004). Each transformed value contained into the dataset was reported as component scores, also called factor scores (Shaw, 2003).

The factor scores were then used to carry out the Hierarchical Cluster Analysis (HCA). This analysis was performed to gather all treatments producing phenotypes that were considered to be similar in groups, named clusters, on the basis of the Euclidean distances measured among the factor scores that were associated with each treatment. Clusters have been filled using the agglomerative method described by Joe H. Ward Jr., also known as Ward's minimum variance criterion methods, or more simply, the Ward method (Shi et al., 2013).

Statistical analysis

Information regarding the cytotoxic effects, the number of spots per cell and size of spots for both lysosomes and LC3B proteins that resulted from the image analysis were repeated three times, then expressed as median values and relative error. For all datasets, the statistical analyses were carried out by applying a one-way ANOVA test through Prism7 software (©1994-2017 GraphPad Software, Inc.), with the confidence interval set at 95% in order to evaluate the p-values relative to the entire data set, and to the data describing each sample, alone and with respect to the data describing the control sample.

Flow-chart

A flow-chart was provided in order to allow a better understanding of the entire experiment and its consecutive steps (Figure 1).

RESULTS AND DISCUSSION

Fluorescence assays on treated SH-SY5Y cells

Fluorescence and immunofluorescence assays were carried out to analyze the effects produced by the 5 different extracts on the autophagy process using SH-SY5Y as the cell model. The effects were analyzed by administering the samples under both physiological and starvation induced conditions. This was also performed by acquiring images demonstrating the effects produced on autophagosomal and acidic compartments that were considered to be descriptive of autophagic activity (Levine and Kroemer, 2008; Lin and Baehrecke, 2015; Molyneux et al., 2007; Shintani and Klionsky, 2004), 2 and 20 h after their administration. This allowed a complete evaluation of the ability of the treatments to induce or inhibit autophagy during shorter and longer periods of time by following and readapting protocols suggested in literature (Levine and Kroemer, 2008; Lin and Baehrecke, 2015). Images obtained from fluorescence and immunofluorescence assays were segmented by the software "CellProfiler", following the guidelines reported by Ljosa and Carpenter (2009) in order to develop a pipeline, through which the cellular elements necessary in describing autophagy (such as nuclei, cells, lysosome and LC3B protein spots) were determined. Such elements have been identified as "objects" by setting up characteristic reference parameters regarding, for example, the intensity assigned to each pixel and the minimum and maximum diameters (Pierzyńska-Mach et al., 2014; Xia, 2011). To extrapolate the quantitative data to the parameters related to the characteristics used to identify the autophagic phenotypes, these objects were then analyzed based on the affection produced by the activity of the extracts on the autophagy pathway. The cellular "objects" and their features describing autophagy are shown in Table 1 and are described hereafter.

Nuclei representing living cells, determined from the

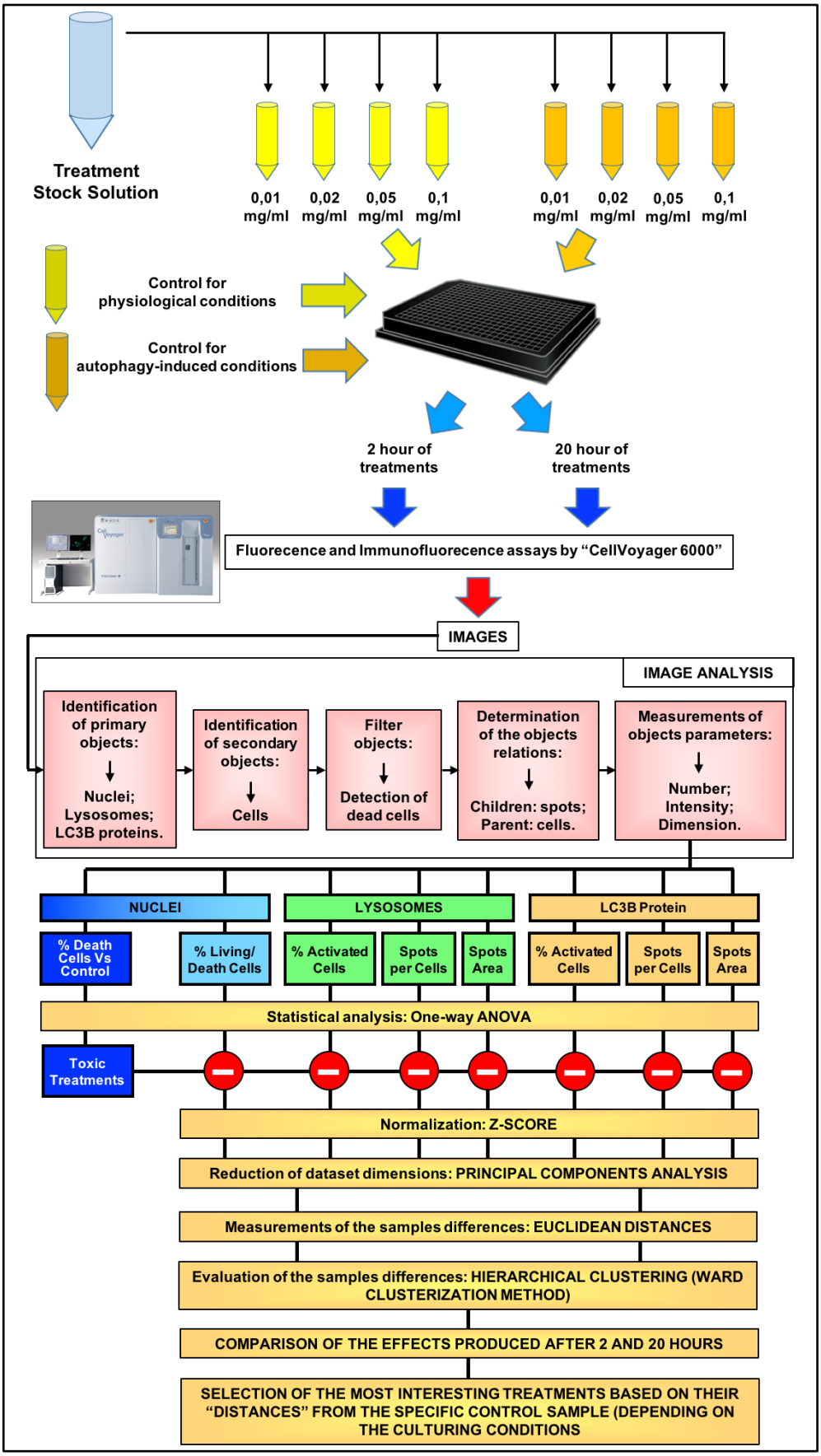

Figure 1: Flow-chart of the experiment.

Table 1: Reference images reporting examples of the features detected during the image analysis of live (images A, B and C) and dead (D, E and F) cells.

	NUCLEI - Hoechst 33342	LYSOSOMES - Lysotracker Red	Hoechst 33342+ Lysotracker Red
SH-SY5Y Lysosomes	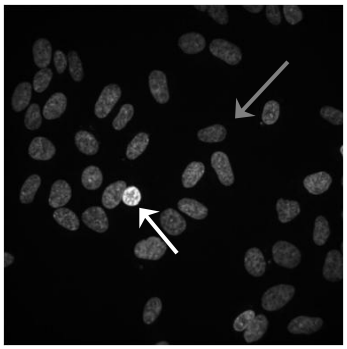 **A**	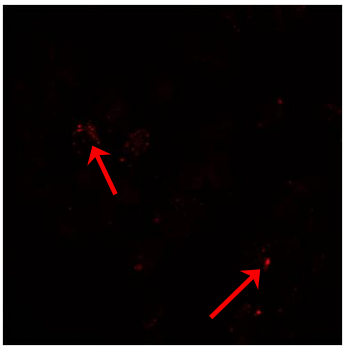 **B**	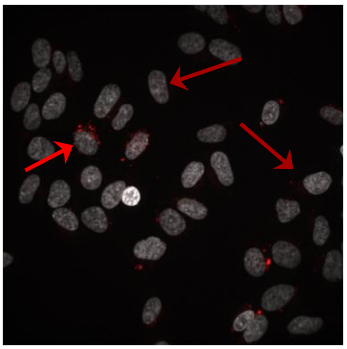 **C**
	Living/Dead Cells	**Lysosomes/LC3B proteins** **- Different Sizes**	**Lysosomes/LC3B proteins** **- Number per cell** **- Activated/Not Activated cells**
SH-SY5Y LC3B proteins	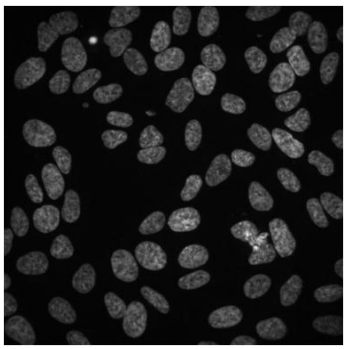 **D**	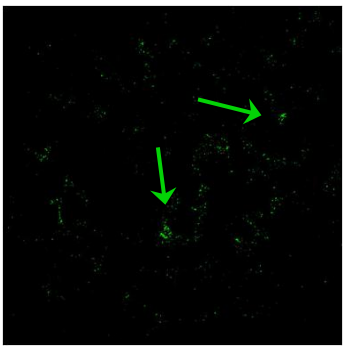 **E**	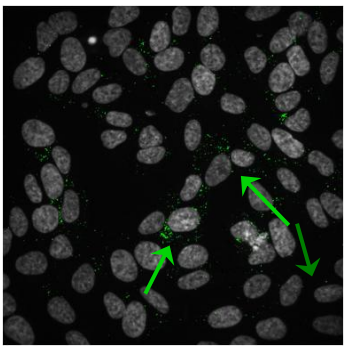 **F**
	NUCLEI - Hoechst 33342	LC3B PROTEINS - Alexafluor488	Hoechst 33342+ Alexafluor488

The grey arrows in image A underline examples of live and dead cells; the red and green arrows in images B and E highlight the different sizes of Lysosome/LC3B protein spots; the red and green arrows in images C and F show the Lysosome/LC3B protein spots counted per cell (light red/green arrows), the cells considered to be active for containing at least one spot (light red/green arrows), and those considered to be inactive for not containing any spots (dark red/green arrows).

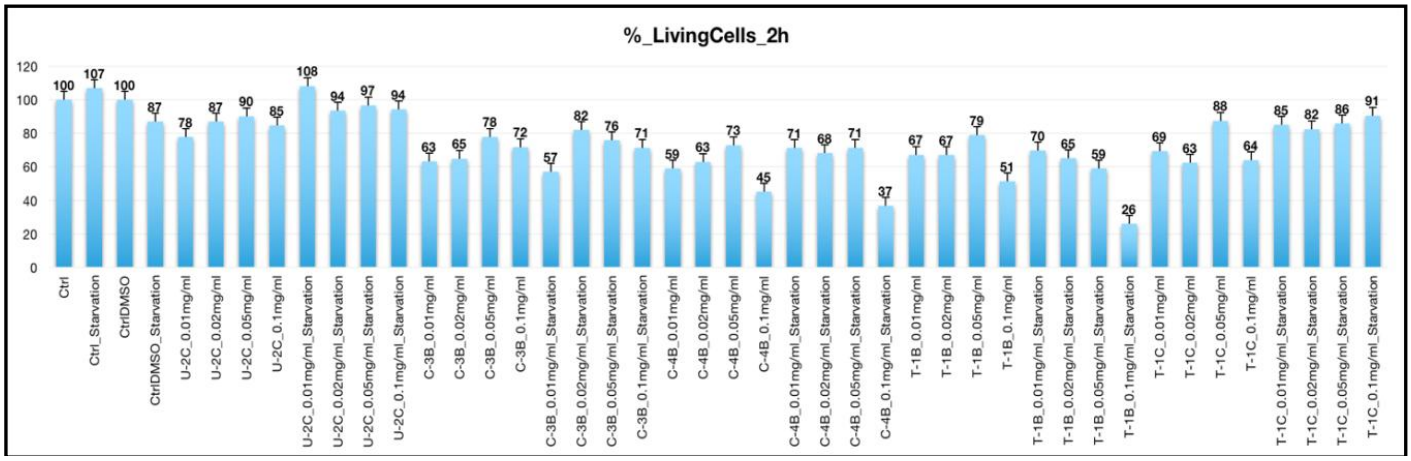

Figure 2: Bar plots reporting the percentages of living cells calculated for each treatment 2 hours after their administration.

images regarding live cells, were selected by applying a raw critical threshold value, arbitrarily chosen, to the median intensity values calculated for each nucleus considering all pixels identifying each object. Nuclei whose median intensity was greater than the threshold were considered to belong to dead cells or to cells that are going to die. Figures A and D in Table 1 report examples of nuclei that identify living (grey arrow) and dead cells (white arrow). Different features related to lysosomes and LC3B proteins were also evaluated, based on the information reported in the literature. The percentage of cells in which the autophagy process activates were measured considering the number of cells containing at least one lysosome/LC3B protein spot related to the total number of the detected living cells. This was reflected by the activation of the acidic/autophagic compartment, respectively, the number of the spots per cell, and the size of the spots, which were measured considering the number of the pixels contained in each determined spot (Lin and Baehrecke, 2015). Examples of such objects and their relative features are reported in figures B, C, E and F in Table 1 (green and red arrows). The subsequent analyses were then performed considering the median values calculated from each of the starting measurements pool of each feature. The median values had been used in order to limit the drift effects caused by possible outlier values due to artifacts or other imperfections that occurred during the staining of the samples. As introduced, the skimming of the samples depending on their toxic power was performed by arbitrarily setting the threshold value at 50%. The treatments were discriminated based on the percentages of living cells calculated, referring to the number of the total cells detected in the control samples. All treatments with measured percentages of living cells lower than 50% were not considered to be interesting, as their toxic activity was too strong. They were therefore discarded before performing the HCA in order to avoid possible inaccurate evaluations regarding their affection of the autophagy process (Shintani and Klionsky, 2004; Yang and Klionsky, 2009; Zanella et al., 2010). The results concerning the toxicity rates that were produced by the treatments after 2 and 20 h were reported as bar plots in Figures 2 and 3: the upper bar plot (Figure 2) shows the percentage of living cells measured after 2 h of treatment administration, while the lower one (Figure 3) reports the percentages measured after 20 h. Upon observing the bar plots, it was found that just 3 samples, more specifically, the highest dilutions of 2 extracts, produced weak toxic action after 2 h: the dilution 0.1 mg/mL *Cryptomenia sp.* (C-4B) administered under both culturing conditions (respectively 45% under physiological conditions and 37% in starvation conditions) and the dilution 0.1 mg/mL *Heliotropium* sp. (T-1B) administered under starvation conditions (26%).

After 20 h, the number of samples that were definitely displaying toxic activity had risen to 13: the dilution 0.1 mg/mL of *Ciona intestinalis* (C-3B) administered under starvation conditions (34%); the dilutions 0.05 and 0.1 mg/mL of *Cryptomenia* sp. (C-4B) administered under both culturing conditions (49 and 14% under physiological conditions and 15 and 1% under starvation conditions, respectively); the dilutions 0.02, 0.05 and 0.1 mg/mL of *Heliotropium* sp. (T-1B) administered under both culturing conditions (26, 2 and 2% under physiological conditions and 6, 3 and 2% under starvation conditions, respectively); the dilution 0.1 mg/mL of *C. intestinalis* (C-3B) administered under both culturing conditions (respectively 10 and 27% under starvation conditions). A deeper analysis reveals that the samples did not produce any evident dose-dependent effect after 2 h. Conversely, the extracts of *C. intestinalis* (C-3B), *Cryptomenia* sp. (C-4B) and the two fractions of *Heliotropium* sp. (T-1B and T-1C) produced a clear dose-dependent effect under both tested culturing conditions 20 h after their administration. The extract of *Ulva* sp. (U-2C) did not show toxic effects on any tested dilution under both culturing conditions, even after 20 h of their administration.

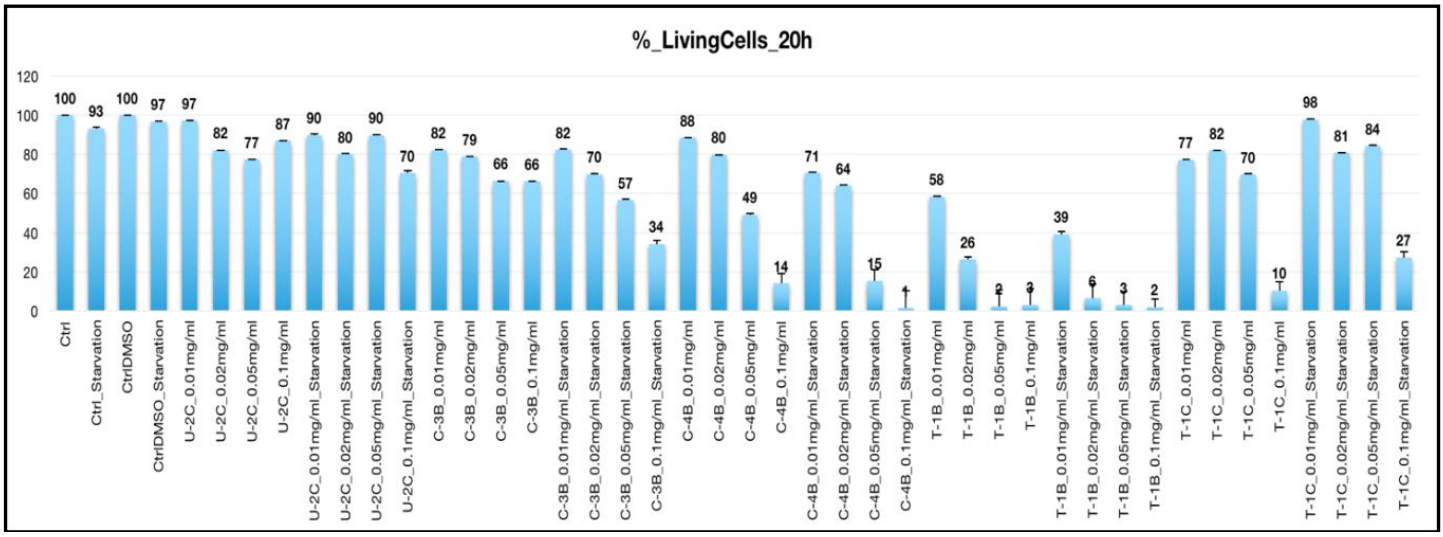

Figure 3: Bar plots reporting the percentages of living cells calculated for each treatment 20 h after their administration.

High content analysis

After the preliminary selection based on the toxicity rate, the remaining samples were subjected to the High Content Analysis (HCA), by which all median values that had been calculated from the datasets, and that contained all measurements of the different features describing of the autophagic activity, were evaluated simultaneously. To reduce the dataset dimensions, the first step of such analysis consisted of performing a PCA, as described previously. The number of the different features describing the autophagic phenotypes was reduced from 7 series of median values (the features described above) to 2 series of factor scores called Principal Component (PC) 1 and 2, through which it was also possible to interpret all future results as if the samples were arranged in a planar space determined by the two PCs as coordinates. The differences among the phenotypes produced by the samples were then evaluated by comparing the Euclidean distances occurring among them, and measured considering the previously calculated factor scores. Based on such distances, samples were collected in different clusters, each of them built following a hierarchical organization based on the "Ward linkage method", so that each of them contained all samples producing the most similar phenotypes (Zang et al., 2012). Based on the results of the Hierarchical Cluster, in order to make the interpretation of the results easier and more complete, Analysis (HCA) of the effects produced on the autophagy pathway by the samples at 2 and 20 h after their administration have been displayed, respectively in Figures 4 and 5, each designed using 3 different elements. In the upper left side, the dendogram resulting from the HCA is included, which reports the disposition (leaf position) and the relative distances (branches length) among all samples. Clusters were identified by cutting the dendogram in order to gather the phenotypes concerning the control samples that were obtained using the same culturing condition in different clusters (Control, Control DMSO, Control Starvation, Control DMSO Starvation). In the lower side of the table, the composition of each cluster has been reported in lists distinguished by differently colored backgrounds, using the same colors that define the clusters in order to make their composition clearer and easier to read. In the upper right side of the tables, the clusters resulting from the HCA have been reported in a scatter plot described by the PCs 1 (x-axis) and 2 (y-axis), with the controls. The most interesting samples were highlighted in order to help their detection; such representation allowed a better evaluation of the distances, as well as the disposition of the samples inside each cluster, defined by planar areas colored as the cluster, thus adding more precise qualitative information to the results showed in the dendogram and reported in the lists.

Concerning the results, at 2 h after the administration, only 9 samples were considered potentially interesting, because they produced effects that differed from both types of control samples (underlined in the list and not highlighted in the scatter plot, but all contained in the green area), while all others were included in the clusters along with the control samples that reproduced the same culturing conditions: samples cultured under physiological conditions with Control and Control DMSO, and samples cultured under starvation conditions with Control Starvation and Control DMSO Starvation.

After 20 h, all phenotypes were grouped along with one of the two control sample types, thus resulting in a total of 2 clusters. From this analysis, only 2 samples were detected to have produced effects considered to be interesting (underlined in the list and highlighted in the scatter plot): the dilutions 0.02 and 0.05 mg/mL of the extract of *C. intestinalis* administered under starvation conditions produced phenotypes similar to those produced by the

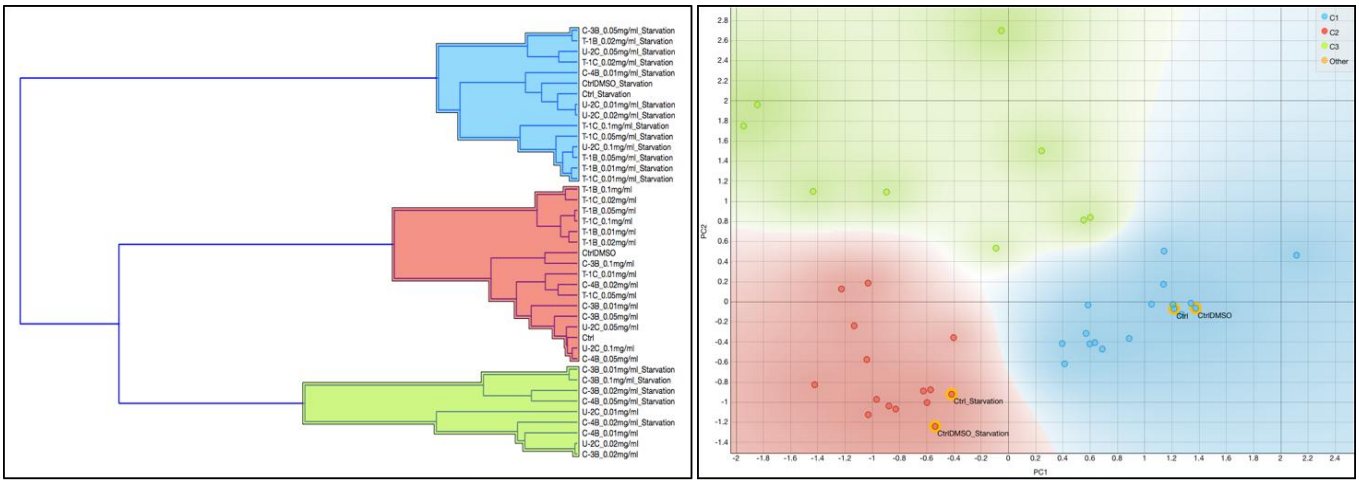

Figure 4: Dendogram, scatter plot and list of the phenotypes produced by the samples 2 h after their administration, divided per cluster after the hierarchical cluster analysis. control samples as well as samples producing effects considered to be interesting were highlighted in order to aid the interpretation of the results.

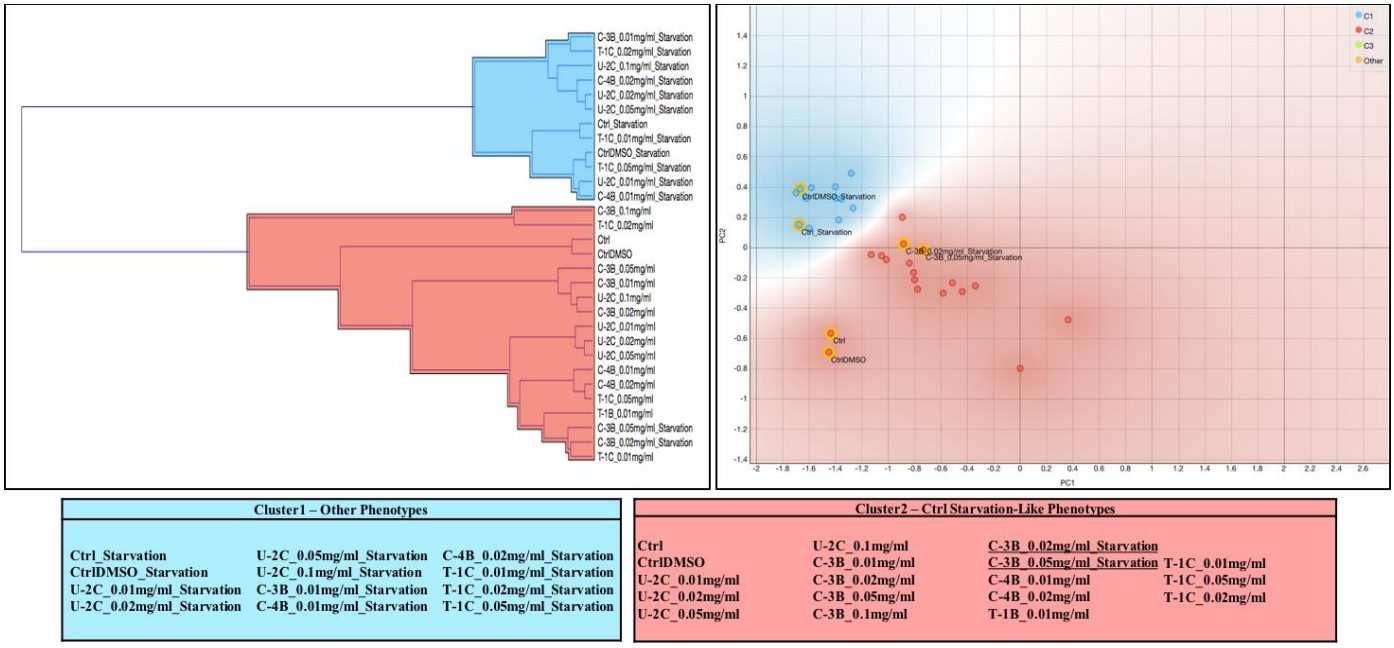

Figure 5: Dendogram, scatter plot and list of the phenotypes produced by the samples 20 h after their administration, divided per cluster after the Hierarchical Cluster Analysis. Control samples as well as samples producing effects considered to be interesting were highlighted in order to aid the interpretation of the results.

control samples under physiological culturing conditions. Hence, such treatments were considered to be potentially able to inhibit or at least to limit the rate of the autophagic activity previously induced by starvation, and thus able to revert the phenotypes to conditions comparable to the physiological. Concerning the spatial distribution of the samples, a careful analysis of the scatter plots (also checking the values of the PC1 and PC2) revealed that the

#	Samples		2 hours treatments								20 hours treatments							
			% l.c.	% l.c. per sample	LYSOSOMES			LC3B			% l.c.	% l.c. per sample	LYSOSOMES			LC3B		
					% Active cells	Per Cell	Area	% Active cells	Per Cell	Area			% Active cells	Per Cell	Area	% Active cells	Per Cell	Area
1	Controls	Ctrl	100	100	79	2	38	100	27	26	100	100	95	16	66	100	84	24
2		CtrlDMSO	107	94	100	7	42	100	53	25	93	100	100	31	66	100	115	23
3		Ctrl starv.	100	100	76	2	38	100	52	25	100	100	93	17	67	100	98	24
4		CtrlDMSO starv.	87	93	100	8	42	100	81	24	97	100	100	32	68	100	121	23
5	U-2C (mg/mL)	0.01	78	98	79	2	36	9	0	25	97	100	87	5	71	100	79	23
6		0.02	87	100	83	3	37	83	5	26	82	100	89	6	72	100	74	23
7	C-3B (mg/mL)	0.02	65	98	82	3	37	82	4	26	79	100	83	4	76	100	48	24
8		0.01 starv.	57	97	100	8	41	22	0	28	82	100	100	22	70	100	36	25
9		0.02 starv.	82	97	96	8	41	37	0	26	70	100	92	12	73	100	55	24
10		0.05 starv.	76	98	97	9	42	65	4	26	57	100	88	11	75	100	64	24
11		0.1 starv.	71	99	90	9	43	1	0	28	34	95	93	20	82	100	126	23
12	C-4B (mg/mL)	0.01	59	100	81	3	37	57	1	27	88	100	96	10	70	100	83	23
13		0.05	73	100	77	2	37	100	26	26	49	100	94	10	80	100	124	21
14		0.1	45	100	65	1	37	100	23	26	14	100	73	8	90	100	101	21
15		0.02 starv.	68	98	92	4	38	81	6	28	64	100	100	23	74	100	103	22
16		0.05 starv.	71	96	96	6	39	71	2	29	15	100	100	16	91	100	110	22
17		0.1 starv.	37	73	95	4	39	60	1	30	1	100	0	0	221	0	0	38
18	T-1B (mg/mL)	0.02	67	98	92	4	39	100	32	26	26	100	100	14	84	100	200	21
19		0.05	79	97	90	3	39	100	32	26	2	50	0	0	110	0	0	28
20		0.1	51	89	85	3	43	100	47	25	3	100	40	0	91	0	0	/
21		0.01 starv.	70	96	100	9	44	100	26	26	39	98	100	30	78	100	180	22
22		0.02 starv.	65	91	98	7	43	87	4	28	6	53	95	9	93	77	25	24
23		0.05 starv.	59	88	100	7	44	100	35	27	3	100	25	0	110	0	0	33
24		0.1 starv.	26	71	94	6	47	96	14	26	2	100	0	0	141	0	0	89
25	T-1C (mg/mL)	0.1	64	98	88	4	38	100	34	26	10	80	100	19	68	100	136	21
26		0.1 starv.	91	99	100	11	45	91	5	28	27	100	100	27	74	100	74	22

Figure 6: Treatments producing interesting activities 2 and 20 h after their administration are reported along with the values of the features considered to be descriptive of autophagic activity (the acronym "l.c." means "living cells"), and are encoded by colored backgrounds. Toxic treatments were reported with a grey background, treatments able to revert from the starvation induced autophagy conditions to the physiological conditions were reported with a red background, and treatments producing phenotypes different from both of the reference control phenotypes were reported with a light blue background. The samples reported with a white background didn't show any interesting activity.

phenotypes tend to be sparser at 2 h after the administration, and tend to become similar to what is produced by the control samples during that time. Another important aspect of this analysis must be highlighted: the two samples considered to be the most interesting were localized very closely to the boundary of the area that was covered by the cluster containing the control samples, reproducing phenotypes representative of the same culturing conditions used for their administration. This suggests that such phenotypes were not significantly different from their standard conditions, and that the reversing effects were very weak.

Comparison of the effects produced 2 and 20 h after the administration of theextracts

Here, the results obtained from the previous investigations, summarized in Figure 6, will be further analyzed. The comparison of the results concerning the effects produced by the treatments 2 and 20 h after their administration show clearly that the number of the treatments considered to be interesting fell to approximately half of the starting number of the analyzed samples (from 40 to 22), including dilutions of all 5 extracts analyzed. More specifically, 10 of the 22 samples considered to be interesting were selected because they affect the autophagy process, while the other 14 were considered potentially interesting due to the toxicity effect caused 2 and/or 20 h after the administration. Among the samples affecting the autophagy process, 9 were selected because they produced an effect that differed from both control samples after 2 h, but changed their effects over time: after 20 h after the administration, 6 of them were no longer considered to be interesting because they produced effects similar to the respective control samples (0.01 and 0.02 mg/mL *Ulva* sp.,

0.02 mg/mL *Cryptomenia* sp., 0.01 mg/mL *Cryptomenia* sp. under starvation conditions, 0.01 mg/mL *C. intestinalis* and 0.02 mg/mL *C. intestinalis* under Starvation conditions) and 2 of them became toxic (0.1 mg/mL *Cryptomenia sp.* in starvation conditions and 0.05 mg/mL *C. intestinalis* in starvation conditions). Only the dilution 0.02 mg/mL of *Cryptomenia sp.* administered in starvation conditions produced a new phenotype comparable to what was produced by the control samples for physiological conditions. By virtue of this evidence, the dilution 0.02 mg/mL starvation of *Cryptomenia* sp. was considered to be interesting for further investigation in order to verify the results and to learn more about its ability to inhibit the autophagy process, or at least to revert the physiological autophagy rate. The only remaining sample among those that affect autophagy process was represented by the dilution 0.05 mg/mL of *C. intestinalis* administered under starvation conditions, which inhibited the autophagy process or reverted the physiological conditions after 20 h, but did not show any interesting activity 2 h after administration. As regards the 14 samples that became toxic after 20 h, most of them had different effects 2 h after their administration. In fact, only 3 of them had already become toxic after 2 h (0.1 mg/mL *C. intestinalis*; 0.1 mg/mL starvation *C. intestinalis*; 0.1 mg/mL starvation *Heliotropium sp.* fraction T-1B). On the basis of such evidence, they were supposed to contain compounds with a strong toxic power, which may be interesting for future studies focused on the discovery of new drugs against diseases such as cancer. Among the remaining 11 toxic samples, at 20 h after their administration, only 2 of them remained potentially interesting for their effects produced on the autophagy process (different from the control samples for both autophagy induced and physiological conditions – 0.1 mg/mL starvation *Cryptomenia sp.*; 0.05 mg/mL *C. intestinalis*), while the other 9 were not found to be interesting for any activity 2 h after their administration (0.05 mg/mL *C. intestinalis*; 0.02, 0.05 and 0.1 mg/mL *Heliotropium sp.* fraction T-1B; 0.01, 0.02 and 0.05 mg/mL *Heliotropium sp.* fraction T-1B; 0.1 mg/mL *Heliotropium sp.* fraction T-1B; 0.1 mg/mL starvation *Heliotropium sp.* fraction T-1B).

Conclusion

In conclusion, the analysis of the effects produced by the samples on the autophagy process, performed through a HCA developed and fine-tuned specifically for this purpose, have allowed the selection of extracts and their relative dilutions that have demonstrated interesting activities. The method presented in this study, that was used to examine raw plant extracts, allows speculation that any substance able to interfere with the autophagy process under pathological conditions may be a good starting point for discovering other potential candidates for drug development programs. More specifically, the HCA reduced the number of samples to approximately half of the starting amount. The phenotypes produced by the treatments were determined by analyzing datasets of the measurements of the seven different features regarding Nuclei, Lysosomes and LC3B proteins, which were chosen because they were considered to be descriptive of autophagic activity. The analysis consisted of the evaluation of the effects produced by the samples through the comparison of the Euclidean distances occurring among the factor scores. The parameters were obtained from the reduction of the dataset dimensions through the PCA, which reliably reproduced the variance contained inside them in a form that was easier to handle, thus making the analysis easier to perform. The autophagy inhibition properties demonstrated by the two selected treatments are good starting points in the search form olecules or molecular phytocomplexes that are able to revert the autophagy process.

In addition to narrowing down the most interesting samples and selecting those with the most interesting activities, the protocol developed and used during this study to analyze the effects of raw natural extracts, consisting of fluorescence and immunofluorescence assays followed by the High Content Analysis of the obtained images, represents a useful tool for future studies. Particularly, this approach provides a potent tool that can be used to screen biological effects of large libraries of raw natural extracts or pure compounds. Moreover, it is also possible to rearrange or adapt such protocol in order to perform similar studies based on the same biological and chemical tools and technologies and with similar biological aims, independent from the samples analyzed, changing, for example, the markers, the analyzed parameters or the cell model.

ACKNOWLEDGMENT

This work was supported by Basal Project PFB- 27.

REFERENCES

Abdi H (2010). Multivariate Analysis. In Encyclopedia of Social Sciences Research Methods, Lewis-Beck, M., Bryman, A., Futing, T., Eds.; SAGE Publications: SAGE: Thousand Oaks, California, USA. pp. 1-4; doi:10.4135/9781412950589.n607.

Abraham VC, Taylor DL, Haskins JR (2004). High content screening applied to large scale cell biology. Trends Biotechnol. 22(1): 15–22.

Alessi DR, Downes CP (1998). The role of PI 3-kinase in insulin action. Biochim Biophys Acta. 1436(1-2): 151-164.

Arroyo DS, Gaviglio EA, Peralta Ramos JM, Bussi C, Rodriguez-Galan MC, Iribarren P (2014). Autophagy in inflammation, infection, neurodegeneration and cancer. Int. Immunopharmacol.18(1): 55-65.

ATCC (2014). Available online: https://www.lgcstandards-atcc.org/Products/All/CRL-2266.aspx.

Bhutia SK, Mukhopadhyay S, Sinha N, Das DN, Panda PK, Patra SK, Maiti TK, Mandal M, Dent P, Wang XY, Das SK, Sarkar D, Fisher PB (2013). Autophagy: cancer's friend or foe? Adv. Cancer Res. 118: 61-95.

Bravo-San Pedro JM, Kroemer G, Galluzzi L (2017). Autophagy and mitophagy in cardiovascular diseases. Circ. Res. 120(11): 1812-1824.

Carnero A (2006). High throughput screening in drug discovery. Clin. Transl. Oncol. 8(7):482-490.

Carpenter AE, Jones TR, Lamprecht MR, Clarke C, Kang IH, Friman O, Guertin DA, Chang JH, Lindquist RA, Moffat J, Golland P, Sabatini DM (2006). Cell Profiler: image analysis software for identifying and quantifying cell phenotypes. Genome Biol. 7(10):R100. doi: 10.1186/gb-2006-7-10-r100.

Cuervo AM (2004). Autophagy: In sickness and in health. Trends Cell Biol. 14(2):70-77.

De Vorkin L, Gorski SM (2014). LysoTracker staining to aid in monitoring autophagy in Drosophila. Cold Spring Harb. Protoc. 2014(9): 951-958.

Dewick PM (2009). Medicinal Natural Products: A biosynthetic approach, 3rd edn.; John Wiley & Sons: West Sussex, UK, 2009. Print ISBN: 9780470741689; Online ISBN: 9780470742761.

Eskelinen EL (2008). New insights into the mechanisms of macroautophagy in mammalian cells. Int. Rev. Cell Mol. Biol. 266: 207-247.

Fitzwalter B, Thorbun A (2015). Recent insights into cell death and autophagy. FEBS J. 282(22): 4279-4288.

Geng J, Klionsky DJ (2008). The Atg8 and Atg12 ubiquitin-like conjugation systems in macroautophagy. EMBO Rep. 9(9): 859-864.

Giuliano KA, Haskins JR, Taylor DL (2003). Advances in high content screening for drug discovery. Assay Drug Dev. Technol. 1(4): 565-577.

Glick D, Barth S, Macleod KF (2010). Autophagy: cellular and molecular mechanisms. J. Pathol. 221(1): 3-12.

Gribbon P, Sewing A (2003). Fluorescence readouts in HTS: no gain without pain?. Drug Discov. Today. 8(22): 1035-1043.

Johnston PA, Johnston PA (2002). Cellular platforms for HTS: three case studies. Drug Discov. Today. 7(6): 353-363.

Kabeya Y, Mizushima N, Ueno T, Yamamoto A, Kirisako T, Noda T, Kominami E, Ohsumi Y, Yoshimori T (2000). LC3, a mammalian homologue of yeast Apg8p, is localized in autophagosome membranes after processing. EMBO J. 19(21): 5720-5728.

Kamentsky L, Jones TR, Fraser A, Bray MA, Logan D, Madden K, Ljosa V, Rueden C, Harris GB, Eliceiri K, Carpenter AE (2011). Improved structure, function, and compatibility for CellProfiler: modular high-throughput image analysis software. Bioinformatics. 27(8): 1179-1180.

Kirisako T, Ichimura Y, Okada H, Kabeya Y, Mizushima N, Yoshimori T, Ohsumi M, Takao T, Noda T, Ohsumi Y (2000). The reversible modification regulates the membrane binding state of Apg8/Aut7 essential for autophagy and the cytoplasm to vacuole targeting pathway. J. Cell Biol. 151(2): 263-276.

Klionsky DJ (2005). The molecular machinery of autophagy: Unanswered questions. J. Cell Sci.118(Pt. 8): 7-18.

Klionsky DJ (2007). Autophagy: From phenomenology to molecular understanding in less than a decade. Nat. Rev. Mol. Cell Biol. 8(11): 931-937.

Klionsky DJ, Abdelmohsen K, Abe A, Abedin MJ, Abeliovich H, Acevedo Arozena A, Adachi H, Adams CM, Adams PD, Adeli K., et al (2016). Guidelines for the use and interpretation of assays for monitoring autophagy (3rd edition). Autophagy. 12(1): 1-222.

Kundu M, Thompson CB (2008). Autophagy: basic principles and relevance to disease. Annu. Rev. Pathol. 3: 427-455.

Lamprecht MR, Sabatini DM, Carpenter AE (2007). CellProfiler: free, versatile software for automated biological image analysis. Biotechniques. 42(1): 71-75.

Levine B, Klionsky DJ (2004). Development by self-digestion: Molecular mechanisms and biological functions of autophagy. Dev. Cell. 6(4): 463-477.

Levine B, Kroemer G (2008). Autophagy in the pathogenesis of disease. Cell. 132: 27-42.

Lin L, Baehrecke E (2015). Autophagy, cell death and cancer. Mol. Cell Oncol. 2(3): e985913.

Ljosa V, Carpenter AE (2009). Introduction to the quantitative analysis of two-dimensional fluorescence microscopy images for cell-based screening. PLoS Comput. Biol. 5(12): e1000603.

Mei Y, Thompson MD, Cohen RA, Tong X (2015). Autophagy and oxidative stress in cardiovascular disease. Biochim. Biophys. Acta. 1852(2): 243-251.

Mishra BB, Tiwari VK (2011). Natural products: an evolving role in future drug discovery. Eur. J. Med. Chem. 46(10): 4769-4807.

Mizushima N, Klionsky DJ (2007). Protein turnover via autophagy: Implications for metabolism. Annu. Rev. Nutr. 27: 19-40.

Mizushima N, Yoshimori T, Levine B (2010). Methods in mammalian autophagy research. Cell. 140(3): 313-326.

Mizushima, N. Methods for monitoring autophagy. Int J Biochem Cell Biol 2004, 36, 2491-2502. doi: 10.1016/j.biocel.2004.02.005.

Molyneux RJ, Mahoney N, Kim JH, Campbell BC (2007). Bioassay-Directed Isolation and Identification of Antiaflatoxigenic Constituents of Walnuts. In Bioactive Natural Products: Detection, Isolation and Structure Determination, 2nd ed.; Colegate, S.M., Molyneux, R.J., Eds.; CRC Press: Boca Raton, Florida. pp. 421-437; ISBN-10: 0-8493-7258-5; ISBN-13: 978-0-8493-7258-2.

Monks A, Scudiero D, Skehan P, Shoemaker R, Paull K, Vistica D, Hose C, Langley J, Cronise P, Vaigro-Wolff A, Gray-Goodrich M, Campbell H, Mayo J, Boyd M (1991). Feasibility of a high-flux anticancer drug screen using a diverse panel of cultured human tumor cell lines. J. Natl. Cancer Inst. 83(11): 757-766.

Nichols A (2007). High Content Screening as a Screening Tool in Drug Discovery. In High Content Screening. Methods in Molecular Biology, Taylor D.L., Haskins J.R., Giuliano K.A., Eds.; Humana Press: New York, USA, 2007; Volume 365; Print ISBN: 978-1-58829-731-0; Online ISBN: 978-1-59745-217-5.

Padmanabhan K, Eddy WF, Crowley JC (2010). A novel algorithm for optimal image thresholding of biological data. J. Neurosci. Methods. 193(2): 380-384.

Petibone DM, Majeed W, Casciano DA (2016). Autophagy function and its relationship to pathology, clinical applications, drug metabolism and toxicity. J. Appl. Toxicol. 37(1): 23-37.

Pierzyńska-Mach A, Janowski PA, Dobrucki JW (2014). Evaluation of acridine orange, LysoTracker Red, and quinacrine as fluorescent probes for long-term tracking of acidic vesicles. Cytometry A. 85: 729-737.

Sezgin M, Sankur B (2004). Survey over image thresholding techniques and quantitative performance evaluation. J. Electron Imaging. 13(1): 146-165.

Shaw PJA (2003). Multivariate statistics for the Environmental Sciences, Hodder-Arnold: London, UK, 2003; ISBN-10: 0340807636; ISBN-13: 9780340807637.

Shi Z, Li CY, Zhao S, Yu Y, An N, Liu Y, Wu C, Yue B, Bao J (2013). A systems biology analysis of autophagy in cancer therapy. Cancer Lett. 337(2): 149-160.

Shintani T, Klionsky DJ (2004). Autophagy in health and disease: A double-edged sword. Science. 306(5698): 990-995.

Ward JH Jr (1963). Hierarchical Grouping to Optimize an Objective Function. J. Am. Stat. Assoc. 58: 236-244.

Xia P (2011). To die or not to die: the role of autophagy in cell death. Aust. Biochem. 42: 14-16.

Yang Z, Klionsky DJ (2009). An overview of the molecular mechanism of autophagy. Curr. Top Microbiol. Immunol. 335: 1-32.

Yonekawa T, Thorbum A (2013). Autophagy and cell death. Essays Biochem. 55: 105-117.

Yoshii SR Mizushima N (2017).. Monitoring and measuring autophagy. Int. J. Mol. Sci. 18(9): 1865.

Zanella F, Lorens JB, Link W (2010). High Content Screening: seeing is believing. Trends Biotechnol. 28(5): 237-245.

Zang R, Li D, Tang I-C, Wang J, Yang S-T (2012). Cell-Based Assays in High-Throughput Screening for Drug Discovery. Int. J. Biotechnol. Wellness Ind. 1: 31-51.